Proceedings of the 21st ICSMGE, Vienna, Austria, 14 – 19 June 2026. Pistrol, Adam & Schweiger (eds.)
Published by: ÖGG, Austrian Society for Geomechanics, Salzburg, Austria, ISBN 978-3-9503898-4-5
https://doi.org/10.53243/ICSMGE2026-2217

Numerical Analysis of Soil Arching with Consideration of Suction Effect

Shun Liu, Chuang Zhao, Xuecheng Bian, Yunmin Chen
Department of Civil Engineering, Zhejiang University, Hangzhou, China, bianxc@zju.edu.cn

Yu-Jun Cui
Laboratoire Navier/CERMES, Ecole Nationale des Ponts et Chaussées, Marne-la-Vallée, France

ABSTRACT: A plane strain trapdoor was analysed by finite-element method with Mohr-Coulomb (MC) model, taking the effect of suction on soil arching into account. The case of sand was considered and the soil arching was defined as the outline of plastic zone above the trapdoor, as opposed to the common methods with assumed soil arch (dimensions and shape). Due to the dilatational behaviour of sand, stress can be transmitted by the interlocks between soil grains, resulting in a triangular or arching plastic zone. When the matric suction is higher than the air-entry value, the apparent cohesion increases with suction decreasing, leading to a reduction in both the height and area of the plastic zone; after a pic value, the apparent cohesion diminishes with further suction decrease, leading to the failure of soil arch. This shows the significant effect of cohesion on soil arching. Moreover, the results obtained reveal that the common limit equilibrium model which assumes a semi-circular soil arch of uniform thickness is suitable only for soils with large dilation angle, while the friction soil arching model of Terzaghi is more suitable for soils with small dilation angle.

KEYWORDS: unsaturated soils, soil arching, Mohr-Coulomb model, air-entry value, plasticity.

1 INTRODUCTION

The term of 'soil arching' has been commonly used to represent the reduction of soil stress between rigid bodies or above tunnels, and the increase of stress on the bodies of higher stiffness (Terzaghi 1943). Because soil arching contributes to reducing the soil surface deformation, it has been wildly considered in the design of pile-supported embankments, retaining walls and tunnel excavation (Lee et al. 2006; Khosravi et al. 2013; King et al. 2019).

Terzaghi (1943) investigated the soil arching phenomenon through trapdoor tests and proposed a related calculation method. Since then, numerous studies have been conducted in this field and partial calculation models were adopted by different countries (GGS 2010; BSI 2012; CRC 2016). Most soil arching models are based on the trapdoor tests. The model of van Eekelen et al. (2013), an extension of the models of Hewlett and Randolph (1988) and Zaeske (2001), shows a good agreement with the experiment. However, only the internal friction angle is considered in the model, ignoring other soil properties such as the dilation angle. The limit equilibrium soil arching models are adopted in the British (BSI 2012), German (GGS 2010) and Dutch (CRC 2016) standards. In these models, the shapes of arches are assumed but the soil cohesion is ignored. The limit state occurs in the entire arch. Pham (2020) modified the limit equilibrium model of Zaeske (2001) by introducing the effect of cohesion as follows: $\sigma_\theta = \sigma_r \cdot K_P + 2c\kappa(K_P)^{0.5}$ where σ_θ is the tangential stress, σ_r is the normal stress, K_P is the passive earth pressure coefficient, c is the embankment cohesion and κ is a cohesion coefficient. Two vertical sliding surfaces were used in the analysis by (Terzaghi 1943), with consideration of both the internal angle and the cohesion.

Basically, as the apparent cohesion changes with matric suction, the soil arching behaviour changes accordingly. Zeng et al. (2018) and Cui et al. (2022) conducted trapdoor tests on sand at different water contents and found that the height of soil arch decreased with the increase of water content. Song et al. (2018) considered different water tables in trapdoor test, and observed that the height of soil arch and the stress on trapdoor were enlarged with the water table rising.

This study aims at numerically investigating the effects of soil properties and matric suction on soil arching. A plain strain trapdoor finite-element analysis with Mohr-Coulomb model was made for this purpose. The plastic zones were determined, allowing not only the evolution of soil arching with suction to be determined, but also the comparison of different soil arching models to be made.

2 PLAIN STRAIN TRAPDOOR FINITE-ELEMENT MODEL

Figure 1 shows a schematic diagram of the finite-element (FE) model, with vertical and bottom boundaries. Based on the conditions of symmetry, the vertical faces of fill were restrained against horizontal movement. The bottom boundaries consisted of two fixed surfaces and one trapdoor surface. A uniform vertical stress ($\sigma_s = \gamma h$) was applied acting upwards to support the fill and represent the trapdoor. The relative movement between particles is an essential requirement for the formation of soil arching, which is achieved by releasing the vertical stress from an initial value equal to 1 kPa at the central surface of the bottom. Moreover, to prevent differential settlement at the upper surface, a minimum height (often critical height) is required, allowing full arching to be developed (van Eekelen and Han 2020). In this analysis, to avoid partial soil arching, the height of fill was three times the trapdoor width, which is greater than the common critical heights (Terzaghi 1943; Hewlett and Randolph 1988).

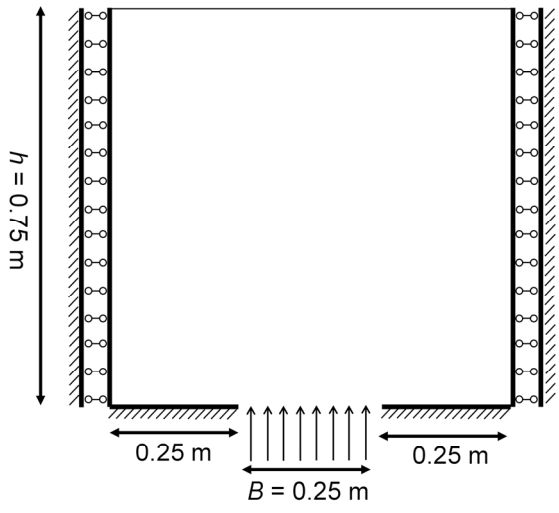

Figure 1. Schematic diagram of the trapdoor model

Soil arching is primarily governed by the strength-controlled development of shear bands/plastic zones, which can be captured transparently using a minimal set of parameters of the Mohr–Coulomb (MC) model (Labuz and Zang 2014). More advanced constitutive models (e.g., Hardening Soil or Barcelona basic model) require additional parameters and coupled hydro-mechanical calibration that are not available for the present parametric study. Therefore, the MC model is considered adequate for revealing the general trends of soil arching with changes in friction, dilation and suction-induced apparent cohesion. Table 1 gives the basic properties of the four saturated sands.

Table 1. Properties of saturated sands

Type	φ (°)	ψ (°)	c (kPa)	γ (kN/m^3)	E (MPa)	μ
1	35	15	2	17	50	0.3
2	35	15	1.5	17	50	0.3
3	35	0	2	17	50	0.3
4	35	0	5	17	50	0.3

In the case of unsaturated soils, the shear strength changes with water content. According to the effective stress concept of Bishop (1959), the shear strength is defined by:

$$\tau = (\sigma - u_a)\tan\varphi' + \chi(u_a - u_w) + c' \quad (1)$$

where σ is the total stress, u_a is the pore air pressure, $u_w u_w$ is the pore water pressure, c' is the effective cohesion, φ' is the internal friction angle and χ is the effective stress parameter.

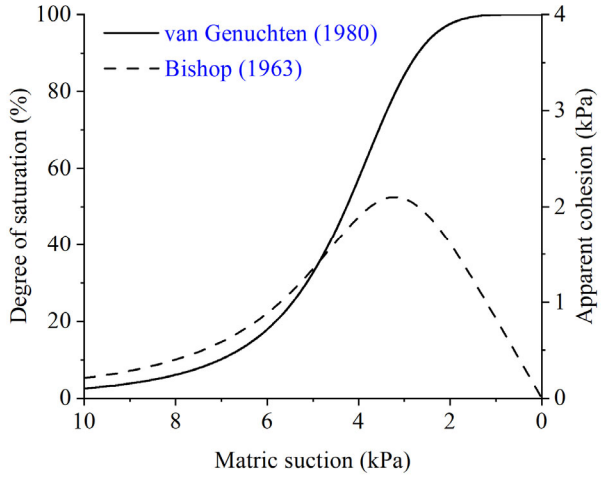

Figure 2. Soil water retention curve and apparent cohesion of Ottawa sand

Table 2. Properties of unsaturated Ottawa sands

$u_a - u_w$ (kPa)	S_r (%)	φ' (°)	ψ (°)	c (kPa)	γ (kN/m^3)	E (MPa)	μ
5	32.65	28.9	16.9	1.35	17	50	0.3
4	57.43	28.9	16.9	1.89	17	50	0.3
3	84.34	28.9	16.9	2.09	17	50	0.3
2	97.57	28.9	16.9	1.61	17	50	0.3
1.5	99.41	28.9	16.9	1.23	17	50	0.3

In order to analyse the effect of suction on soil arching, the unsaturated Ottawa sand (Goulding 2006) was considered. Its water retention curve was described by the van Genuchten model (van Genuchten 1980). Its effective stress parameter (χ) is taken equal to the degree of saturation (S_r) (Bishop and Blight 1963). The influence of suction was embodied by the varying apparent cohesions in the MC model. According to Equation (1), the apparent cohesion was calculated, and shown in Figure 2. It appears that before the air-entry value (about 3 kPa) the apparent cohesion is increasing with suction decrease. However, after the air-entry value, it is decreasing with suction decrease. Five suctions were considered in the analysis, as shown in Table 2.

3 RESULTS

The results of finite element analysis for the four saturated sands are presented in Figure 3. As shown in Figure 3(a), when the effective cohesion is as high as 2 kPa, the plastic zone is triangular and the two plastic bands are not connected, showing that the stress of sands above the center of trapdoor does not reach its shear strength. While the cohesion decreases down to 1.5 kPa (Figure 3(b)), the decrease of shear strength causes plastic strain on the dome of arch, giving rise to a full arch over the trapdoor, with a significant arch height. Comparison between Figure 3(a) and Figure 3(c) shows that the plastic zone of low shear dilatancy is vertical, not triangular or arching, confirming the results of Osman and Jacobsz (2019) and Khatami et al. (2021) which show that the inclination of shear band is approximately equal to the dilation angle with the exception for the area near the free surface and the centerline where the inclination is greater than the dilation angle. Besides, the height of plastic zone with low shear dilatancy is slightly higher than that with large shear dilatancy. Figure 3(c) & (d) reveal that the height of plastic zone is governed by the effective cohesion as well and a larger effective cohesion leads to a lower plastic zone.

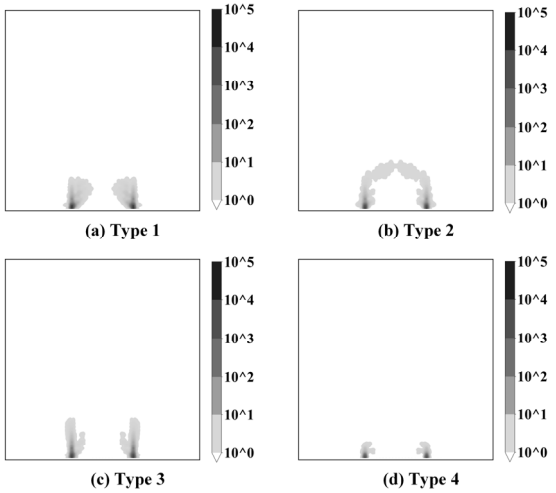

Figure 3. Plastic strains of saturated sands (με)

Figure 4 shows the simulation outputs of vertical displacement, element volume and equivalent plastic strain for different suctions. At suction 5 kPa, the settlement at the upper surface is differential. Prior to reaching the air-entry value, the apparent cohesion increases with the decrease of matric suction. Concurrently, the plastic zone evolves from triangular to arching, leading to a reduction in the heights of equal settlement plane, the volume increasing zone and the plastic zone. Furthermore, the shape of vertical displacement is close to a three-quarter ellipse, and the shape of volume increasing zone is close to a half ellipse. While the friction between soil grains decreases the plastic strain corresponding to the relative movement of grains, the dilatancy increases the unit volume. Besides, the increase of apparent cohesion enhances the shear strength. Thus, less soils above the trapdoor reach the limit state and develop plastic strain, indicating that the areas of volume increasing zone and plastic zone also decreases with suction decreasing. In contrast, the non-plastic area, which is inside the inner outline of plastic zone, increases with suction decreasing. Similar results were obtained by Cui et al. (2022) through trapdoor tests - the soil stress on the trapdoor was reduced with

the increase of water content, indicating that the soil arching is strengthened by water content increase. da Silva Burke (2025) also observed that 10% moisture content (MC) had the highest arch, and not the wettest (MC15) and dryest (MC5) tests. It can be explained that as water is added to the dry soil, capillary bridges that were previously disconnected or confined to the smallest pores begin to expand and merge. The effective contact area between the pore water and the soil particles increases significantly. This increase in the effective wetted area outweighs the reduction in matric suction pressure. Consequently, the net capillary force pulling the grains together increases. The increased apparent cohesion enhances soil strength.

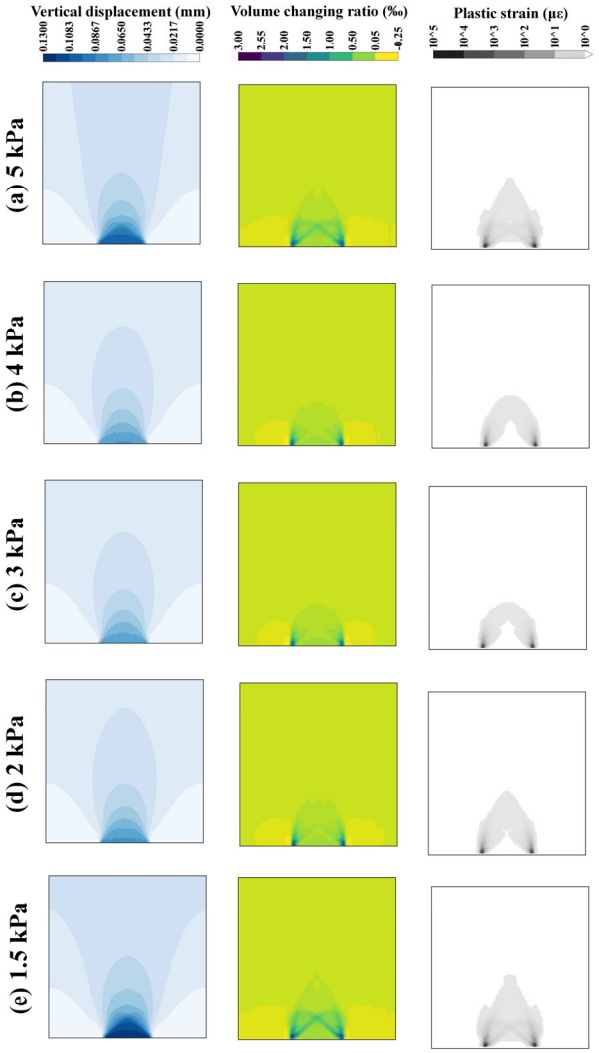

Figure 4. Vertical displacement, volume changing ratio and plastic strain under different suctions

At suction 3 kPa (S_r = 84%), the apparent cohesion of sands reaches the maximum value. Subsequently, as the matric suction decreases and the sand tends to reach fully saturation, the apparent cohesion rapidly diminishes, leading to the failure of soil arching. The variations of soil arch height, the area of volume increasing and plastic strain are opposite to those before the suction reaches 3 kPa, in agreement with the results of Song et al. (2018) obtained from trapdoor tests under different water tables - the height of equal settlement plane of saturated soil is greater than the height of equal settlement plane of dry soil. Liu et al. (2025a) and Liu et al. (2025b) investigated that the effective pile efficacy was pronouncedly reduced by 17% as the water level rose to the critical height of soil arching.

4 DISCUSSIONS

The soil arching phenomenon can be greatly affected by suction through the changes in cohesion. It is worth noting that in case of compacted fine-grained soils, suction can affect the soil aggregate stiffness or deformability, thereby the dilation angle and in turn the arching behaviour. Indeed, Cui and Delage (1996) showed that for a compacted silt the dilation angle increases with the increase of suction. For sand, as the grains stiffness does not change with suction, the dilation angle should be independent of suction. Indeed, for the Ottawa sand, the direct shear results of Goulding (2006) shows that the dilation angle is similar for different water contents. This is the reason why the suction effect on dilation angle is not addressed in this study. Smith et al. (2022) noted that the inclination of the parabolic arch assumed by Engesser (1882) is φ', the same as the failure mechanism assumed by Simon (2013). In the studies of King et al. (2019), the inclination identified experimentally is $\frac{\pi}{2}+\frac{\varphi'+\psi}{4}$. However, when the dilation angle is zero, the geometry of the failure surface cannot be accurately described by these inclinations. Further studies considering all soil parameters are needed to better understand the mechanism of soil arching. It should be emphasised that the present work is a simplified strength-based analysis (MC with suction represented by apparent cohesion), intended to explain general arching mechanisms and trends rather than to reproduce a specific test with full hydro-mechanical coupling. A quantitative calibration/validation against dedicated trapdoor tests and the use of advanced constitutive models for suction-dependent stiffness and collapse behaviour will be addressed in future work.

The existing arching calculation models can be categorized into frictional soil arching models, limit equilibrium soil arching models, and rigid soil arching models (Lai et al. 2018). As shown in Figure 3, the hypothetic arch shapes in rigid and limit equilibrium soil arching models are triangular and arching, respectively, which are the same as for the soils with large dilation angle. Besides, one of the assumptions of Terzaghi model is vertical shear zone, which is more suitable for the soils without dilatational behaviour, such as clay and loose sand. The common problem of the existing models is the height of soil arch is assumed, not variable with soil shear strength.

According to the assumptions of limit equilibrium soil arching model, the arch is semi-circular, of uniform thickness. Also, the static equilibrium condition requires that the radial stress multiplied by Rankine passive earth pressure coefficient equals the tangential stress in the limit. However, the limit equilibrium soil arching model is based on the arching phenomenon in trapdoor tests on non-cohesive soils (Hewlett and Randolph 1988). From the results in the numerical analyses, it appears that the apparent cohesion due to suction can greatly contribute to the soil arching phenomenon. In current models, only Terzaghi model considers the Mohr-Coulomb shear strength including friction angle and cohesion. Hence, in future development of soil arching models, the consideration of the effects of soil properties and suction is important.

5 CONCLUSIONS

This paper presents a simplified plane strain trapdoor analysis with Mohr-Coulomb model by finite-element method, aiming at investigating the effects of soil properties and suction on soil arching which corresponds to the zone of equivalent plastic strain. The obtained results allow the following conclusions to be drawn:

(1) Dilatational behaviour of soils leads to a triangular or arching shape above the trapdoor. When the dilation angle

approaches zero, the plastic zone formed above the trapdoor is vertical, showing the importance of dilation angle in soil arching. The soil cohesion also plays an important role in soil ach development.

(2) For unsaturated sand, before the air-entry value is reached, the apparent cohesion increases with suction decreasing. Concurrently, the plastic zone of the soil arch transitions from triangular to arching as the shear strength increases, leading to a reduction in both the height and area of the plastic zone. At air entry value (3 kPa), the apparent cohesion reaches the maximum value. Then, as the matric suction decreases and the sand tends to saturation, the apparent cohesion diminishes, leading to the failure of the soil arch. This confirms the importance of soil cohesion in soil arching.

(3) The common limit equilibrium model which defines a semi-circular soil arch of uniform thickness is suitable only for soils with large dilatancy, while the friction soil arching model of Terzaghi is more suitable for soils without small dilation angle. The shape and area of plastic zone are not assumed and influenced by the shear strength of soils.

6 ACKNOWLEDGEMENTS

Financial supports from the National Natural Science Foundation of China (52125803) are gratefully acknowledged.

7 REFERENCES

Bishop, A. W. 1959. "The Principle of Effective Stress." *Teknisk Ukeblad*. 39, 859-863.

Bishop, A. W., and Blight, G. 1963. "Some aspects of effective stress in saturated and partly saturated soils." *Geotechnique*. 13(3), 177-197.

BSI. 2012. "Code of practice for strengthened/reinforced soils and other fills." *BS 8006*, B. S. Institution, ed.

CRC. 2016. "Design Guideline Basal Reinforced Piled Embankments." *CUR 226*, C. Press, ed.

Cui, P., Zhu, Y., Liu, Y., Zhu, Z., and Pan, Y. 2022. "Model test and particle flow numerical simulation of soil arching effect for unsaturated sandy soil tunnel." *Rock and Soil Mechanics*. 42(12), 7.

Cui, Y., and Delage, P. 1996. "Yielding and plastic behaviour of an unsaturated compacted silt." *Géotechnique*. 46(2), 291-311.

da Silva Burke, T. "Visualisation of soil arching in unsaturated soils." *Proc., 2nd Southern African Geotechnical Conference*, 433-438.

Engesser, F. 1882. "Über den Erddruck gegen innere Stützwände." *Deutsche Bauzeitung*. 36.

GGS. 2010. "Guideline for the Design and Calculation of Soil Structures with Geosynthetic Reinforcement." *EBGEO*, G. G. S. D. e.V., ed.

Goulding, B. 2006. "Tensile strength, shear strength, and effective stress for unsaturated sand."

Hewlett, W. J., and Randolph, M. F. "Analysis of piled embankments." *Proc., International Journal of Rock Mechanics and Mining Sciences and Geomechanics Abstracts*, Elsevier Science, 297-298.

Khatami, H., Deng, A., and Jaksa, M. 2021. "Mapping soil arching-induced shear and volumetric strains in dense sands." *Transportation Geotechnics*. 28, 100547.

Khosravi, M., Pipatpongsa, T., and Takemura, J. 2013. "Experimental analysis of earth pressure against rigid retaining walls under translation mode." *Géotechnique*. 63(12), 1020-1028.

King, L., Bouazza, A., Dubsky, S., Rowe, R. K., Gniel, J., and Bui, H. H. 2019. "Kinematics of soil arching in piled embankments." *Géotechnique*. 69(11), 941-958.

Labuz, J. F., and Zang, A. (2014). "Mohr–Coulomb failure criterion." *The ISRM Suggested Methods for Rock Characterization, Testing and Monitoring: 2007-2014*, Springer, 227-231.

Lai, H., Zheng, J., Zhang, R., and Cui, M. 2018. "Classification and characteristics of soil arching structures in pile-supported embankments." *Computers and Geotechnics*. 98, 153-171.

Lee, C., Wu, B., Chen, H., and Chiang, K. 2006. "Tunnel stability and arching effects during tunneling in soft clayey soil." *Tunnelling and Underground Space Technology*. 21(2), 119-132.

Liu, S., Bian, X., Cui, Y., and Chen, Y. 2025a. "Full-Scale Experimental Study on the Degradation of Pile-Supported Embankment due to Water Infiltration." *Journal of Geotechnical and Geoenvironmental Engineering*. 151(11), 04025129.

Liu, S., Luo, Z., Zhao, C., Bian, X., Cui, Y., and Chen, Y.-M. 2025b. "Long-term performance of geogrid embedded in railway pile-supported embankment." *Canadian Geotechnical Journal*. 62(1-17).

Osman, A. S., and Jacobsz, S. W. 2019. "Analysis of maximum arching conditions in active plane-strain trapdoors in sand." *Computers and Geotechnics*. 113, 103089.

Pham, T. A. 2020. "Behaviour of piled embankment with multi-interaction arching model." *Géotechnique Letters*. 10(4), 582-588.

Simon, B. 2013. *Recommendations for the design, construction and control of rigid inclusion ground improvements : ASIRI national project*. Presses des Ponts.

Smith, E. J., Bouazza, A., King, L. E., and Rowe, R. K. 2022. "New insights into soil arching behaviour in column-supported embankments." *Canadian Geotechnical Journal*. 59(6), 901-921.

Song, J., Chen, K., Li, P., Zhang, Y., and Sun, C. 2018. "Soil arching in unsaturated soil with different water table." *Granular Matter*. 20, 1-11.

Terzaghi, K. 1943. *1943, Theoretical soil mechanics, Wiley, New York*.

van Eekelen, S., Bezuijen, A., and van Tol, A. 2013. "An analytical model for arching in piled embankments." *Geotextiles and Geomembranes*. 39, 78-102.

van Eekelen, S., and Han, J. 2020. "Geosynthetic-reinforced pile-supported embankments: state of the art." *Geosynthetics International*. 27(2), 112-141.

van Genuchten, M. T. 1980. "A closed‐form equation for predicting the hydraulic conductivity of unsaturated soils." *Soil science society of America journal*. 44(5), 892-898.

Zaeske, D. 2001. *Zur Wirkungsweise von unbewehrten und bewehrten mineralischen Tragschichten über pfahlartigen Gründungselementen*. Fachgebiet u. Versuchsanst. Geotechnik, Univ. Gh Kassel.

Zeng, C., Liang, H., Chen, Q., Zhong, J., You, Z., and Hu, Q. 2018. "Experimental study of the Influence of moisture content on the soil arching in sandy soils." *Soil Engineering and Foundation*. 32(05), 514-516+520.